

The Tig1 Histone Deacetylase Complex Regulates Infectious Growth in the Rice Blast Fungus *Magnaporthe oryzae*

Sheng-Li Ding,^{a,1} Wende Liu,^{a,1} Anton Iliuk,^c Cecile Ribot,^d Julie Vallet,^d Andy Tao,^c Yang Wang,^b Marc-Henri Lebrun,^{d,e} and Jin-Rong Xu^{a,b,2}

^a Department of Botany and Plant Pathology, Purdue University, West Lafayette, Indiana 47907

^b College of Plant Protection and Shaanxi Key Laboratory of Molecular Biology for Agriculture, Northwest A&F University, Yangling, Shaanxi 712100, China

^c Department of Biochemistry, Purdue University, West Lafayette, Indiana 47907

^d Université Lyon-1, Centre National de la Recherche Scientifique, Bayer CropScience, 69263 Lyon Cedex 09, France

^e Institut National de la Recherche Agronomique, 78850 Thiverval-Grignon, France

***Magnaporthe oryzae* is the most damaging fungal pathogen of rice (*Oryza sativa*). In this study, we characterized the *TIG1* transducin β -like gene required for infectious growth and its interacting genes that are required for plant infection in this model phytopathogenic fungus. Tig1 homologs in yeast and mammalian cells are part of a conserved histone deacetylase (HDAC) transcriptional corepressor complex. The *tig1* deletion mutant was nonpathogenic and defective in conidiogenesis. It had an increased sensitivity to oxidative stress and failed to develop invasive hyphae in plant cells. Using affinity purification and coimmunoprecipitation assays, we identified several Tig1-associated proteins, including two HDACs that are homologous to components of the yeast Set3 complex. Functional analyses revealed that *TIG1*, *SET3*, *SNT1*, and *HOS2* were core components of the Tig1 complex in *M. oryzae*. The *set3*, *snt1*, and *hos2* deletion mutants displayed similar defects as those observed in the *tig1* mutant, but deletion of *HST1* or *HOS4* had no detectable phenotypes. Deletion of any of these core components of the Tig1 complex resulted in a significant reduction in HDAC activities. Our results showed that *TIG1*, like its putative yeast and mammalian orthologs, is one component of a conserved HDAC complex that is required for infectious growth and conidiogenesis in *M. oryzae* and highlighted that chromatin modification is an essential regulatory mechanism during plant infection.**

INTRODUCTION

The ascomycetous fungus *Magnaporthe oryzae* is the causal agent of rice blast, which is one of the most destructive fungal diseases of rice (*Oryza sativa*) throughout the world (Dean et al., 2005; Wilson and Talbot, 2009). It produces three-celled pyriform conidia for dispersal. The infection process is initiated with the attachment and germination of conidia on the plant surface. An appressorium, a highly specialized infection structure, forms at the tip of the germ tube and penetrates the plant cuticle and cell wall (Tucker and Talbot, 2001). After penetration, the fungus forms unbranched primary invasive hyphae, which in turn differentiate into bulbous invasive hyphae. *M. oryzae* is a hemibiotrophic fungus that does not kill infected plant cells during the early stages of infection. Invasive hyphae are enclosed within the host cell membrane (Kankanala et al., 2007). Although it is not

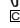
clear when necrotrophic growth begins, plant cells eventually die due to infectious growth of *M. oryzae*. Abundant conidia are produced on lesions that develop on rice plants during the late stages of infection to reinitiate the infection cycle. Under suitable conditions, infected seedlings can be killed by infection with *M. oryzae*, and panicle blast can cause severe yield losses.

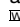
The *M. oryzae*–rice pathosystem is a model system for studying fungal–plant interactions. In the past decade, there have been extensive studies on the molecular mechanisms that regulate appressorium morphogenesis and penetration in *M. oryzae* (Zhao et al., 2007; Wilson and Talbot, 2009). In addition to *ALB1*, *BUF1*, and *RSY1*, which are required for melanin synthesis, many genes that are important for appressorium formation and penetration have been characterized (Ebbole, 2007; Xu et al., 2007), including *PTH12*, *MMT1*, *TPS1*, *CYP1*, *PLS1*, *MIG1*, and *MHP1* (Clergeot et al., 2001; Tucker et al., 2004; Wilson et al., 2007; Mehrabi et al., 2008; Kim et al., 2009). Among these genes found to be important for early plant infection processes are several components of cAMP signaling and two mitogen-activated protein (MAP) kinase pathways. In *M. oryzae*, the cAMP-PKA pathway regulates the recognition of hydrophobic surfaces and initiation of appressorium formation (Mitchell and Dean, 1995; Fang and Dean, 2000). The Pmk1 MAP kinase pathway is required for appressorium formation and maturation (Zhao et al., 2007). It is also essential for root infection (Sesma and Osbourn, 2004) and the proper regulation of the mobilization of

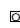
¹ These authors contributed equally to this work.

² Address correspondence to jinrong@purdue.edu.

The author responsible for distribution of materials integral to the findings presented in this article in accordance with the policy described in the Instructions for Authors (www.plantcell.org) is: Jin-Rong Xu (jinrong@purdue.edu).

 Some figures in this article are displayed in color online but in black and white in the print edition.

 Online version contains Web-only data.

 Open Access articles can be viewed online without a subscription. www.plantcell.org/cgi/doi/10.1105/tpc.110.074302

storage carbohydrate and lipid reserves from conidia to appressoria (Thines et al., 2000). The other MAP kinase pathway essential for pathogenesis in *M. oryzae* is the *MPS1* cascade, which is dispensable for appressorium formation but required for appressorial penetration (Xu et al., 1998; Jeon et al., 2008; Mehrabi et al., 2008). These two pathways also have been shown to be important for plant infection in other phytopathogenic fungi, including some species that do not form appressoria (Rispaill et al., 2009).

Compared with our knowledge of appressorium formation and penetration, our knowledge of the molecular mechanisms involved in the differentiation and growth of invasive hyphae in infected plant cells is limited. Although several genes are known to be important for infectious growth in planta (for reviews, see Ebbole, 2007; Xu et al., 2007; Wilson and Talbot, 2009), most of them, such as the *PMK1* MAP kinase and *PDE1* P-type ATPase genes, also are involved in other developmental and infection processes. The corresponding mutants normally have pleiotropic defects. Only a few mutants, including the *abc1*, *des1*, and *pth8* mutants, have no obvious defects in growth and appressorium-mediated penetration but are defective in plant infection. These genes must have cellular functions that are specific for invasive hyphae, such as the *ABC1* transporter gene for avoiding toxic plant defense compounds (Urban et al., 1999) and *DES1* for suppressing the plant defense response (Chi et al., 2009). Recently, microarray analysis has been used to identify genes specifically or highly expressed in invasive hyphae (Mosquera et al., 2009). Many of these genes expressed in planta have never been detected in vitro and encode biotrophy-associated secreted (BAS) proteins. Some, but not all, BAS proteins localize to biotrophic interfacial complexes (Mosquera et al., 2009). Because none of the BAS genes that have been functionally characterized are essential for pathogenicity (Mosquera et al., 2009), their functions in plant colonization and infectious growth are not clear.

In the wheat scab fungus *Fusarium graminearum*, the *TBL1*-like gene *FTL1* was identified as a novel fungal pathogenicity factor by random insertional mutagenesis (Ding et al., 2009). *FTL1* encodes a protein that is putatively orthologous to yeast *SIF2* and mammalian *TBL1*. The *ftl1* mutant was nonpathogenic. However, the molecular mechanism underlying its defects in plant infection is not clear. Because its infection processes, particularly fungal-plant interactions after plant penetration, are not well understood, *F. graminearum* is not suited for detailed characterization of this novel pathogenicity factor. In this study, we identified and characterized the *TIG1* gene, an *FTL1* ortholog, in the model plant pathogenic fungus *M. oryzae*. The *tig1* mutant formed appressoria but was nonpathogenic. It was defective in the differentiation and growth of invasive hyphae in planta. The mutant had increased sensitivities to oxidative stress and other plant defensive compounds. Using affinity purification and mass spectrometry analyses, we identified several Tig1-associated proteins that are homologous to components of the yeast Set3 complex, including two histone deacetylases (HDACs). Coimmunoprecipitation assays were used to confirm the interactions among Tig1, Snt1, Set3, and Hos2. Mutants lacking any one of these genes had similar defects in plant infection and conidiation. HDAC activities and histone acetylation levels were also affected in these mutants disrupted in the Tig1 complex. Our

data indicate that Tig1 is a component of a well-conserved HDAC complex and that chromatin modification is an essential regulatory mechanism during plant infection.

RESULTS

Identification of the *TIG1* Transducin β -Like Gene in *M. oryzae*

In the *M. oryzae* genome, MGG_03198.5 shares >50% amino acid identity with *F. graminearum* *FTL1* and yeast *SIF2*. It has an N-terminal LisH domain (residues 6 to 38) and six WD40 repeats (residues 536 to 626) toward the C terminus. The cDNA of *TIG1* (for *TBL1*-like gene required for invasive growth) was amplified and sequenced. Four predicted introns in the *TIG1* coding region were confirmed by sequence analysis. Although no known protein domain was identified, the amino acid sequence between the LisH domain and WD40 repeats was conserved between *TIG1* and its orthologs from *Neurospora crassa* and *F. graminearum* (see Supplemental Figure 1 online).

To determine the function of *TIG1* in *M. oryzae*, a gene replacement construct (Figure 1A) was obtained by ligation-PCR and transformed into Guy11 (Chao and Ellingboe, 1991). The resulting hygromycin-resistant transformants were screened by PCR and analyzed by DNA gel blot hybridization. When hybridized with a *TIG1* fragment, a 3.6-kb *Pst*I band was observed in the wild type but not in the *tig1* deletion mutant strains (Figure 1B). When hybridized with the hygromycin phosphotransferase gene (*hph*), the *tig1* mutant but not the wild type had an 11.1-kb band that was characteristic of the gene replacement event (Figure 1B). The *tig1* mutant KT-1 (Table 1) grew slightly slower than the wild type but

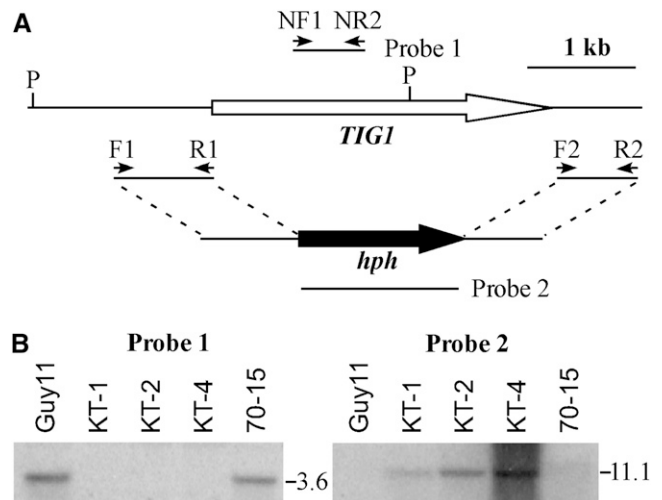


Figure 1. The *TIG1* Gene Replacement Construct and Mutants.

(A) Schematic diagram of the genomic region of the *TIG1* and *hph* genes. Primers F1, R1, F2, R2, NF1, and NR1 were used to generate the *TIG1* gene replacement constructs and mutant screens. P, *Pst*I.

(B) DNA gel blots of *Pst*I-digested genomic DNA were hybridized with a *TIG1* fragment (left panel) and the *hph* gene (right panel) as the probes. Guy11 and 70-15 are the wild-type strains. KT-1, KT-2, and KT-4 are three independent *tig1* null mutants.

Table 1. Wild-Type and Mutant Strains of *M. oryzae* Used in This Study

Strain	Genotype Description	Reference
Guy11	Wild-type (<i>MAT1-2</i> , <i>avr-Pita</i>)	Chao and Ellingboe (1991)
70-15	Wild-type (<i>MAT1-1</i> , <i>AVR-Pita</i>)	Chao and Ellingboe (1991)
Ku80	<i>MgKu80</i> deletion mutant of Guy11	Villalba et al. (2008)
KT-1	<i>tig1</i> deletion mutant of Guy11	This study
KT-2	<i>tig1</i> deletion mutant of 70-15	This study
KT-4	<i>tig1</i> deletion mutant of 70-15	This study
ECT23	Ectopic transformant of Guy11	This study
CT-1	KT-1 transformant complemented with <i>TIG1</i>	This study
KT1NG1	KT-1 transformant expressing the <i>TIG1</i> -GFP construct	This study
TigRG1	70-15 transformant expressing P _{RP27} - <i>TIG1</i> -GFP	This study
KT1RG1	KT-1 transformant expressing P _{RP27} - <i>TIG1</i> -GFP	This study
TFg1	70-15 transformant expressing <i>TIG1</i> -3xFLAG fusion	This study
SetG1	70-15 transformant expressing <i>SET3</i> -GFP fusion	This study
HosG1	70-15 transformant expressing <i>HOS2</i> -GFP fusion	This study
TS-29	<i>TIG1</i> -3xFLAG and <i>SET3</i> -GFP transformant	This study
HT-26	<i>TIG1</i> -3xFLAG and <i>HOS2</i> -GFP transformant	This study
HS-9	<i>SET3</i> -3xFLAG and <i>HOS2</i> -GFP transformant	This study
KH2-13	<i>hos2</i> deletion mutant of 70-15	This study
CH-1	<i>hos2/HOS2</i> complementation strain of KH2-13	This study
KH4-81	<i>hos4</i> deletion mutant of 70-15	This study
KH1-23	<i>hst1</i> deletion mutant of 70-15	This study
ECT1	An ectopic transformant of 70-15	This study
KS1-1	<i>snt1</i> deletion mutant of Ku80	This study
KS3-1	<i>set3</i> deletion mutant of Ku80	This study
CS-1	<i>set3/SET3</i> complementation strain of KS3-1	This study
ECT2	An ectopic transformant of Ku80	This study

was significantly reduced in conidiation. In comparison with Guy11, KT-1 produced ~100-fold fewer conidia (Table 2).

The *tig1* Deletion Mutant Is Defective in Plant Infection

When seedlings of rice cultivar CO-39 were spray inoculated with conidia from Guy11 and an ectopic transformant, abundant lesions formed (Figure 2A). On leaves inoculated with the *tig1* mutant KT-1, no typical blast lesions were observed, but small dark brown spots were formed occasionally (Figure 2A). Similar results were obtained in infection assays with seedlings of barley (*Hordeum vulgare*) cultivar Golden Promise. The *tig1* mutant failed to cause blast lesions and green islands on barley leaves. In injection infection assays, only limited necrosis was observed at the wound sites inoculated with KT-1 (Figure 2B). When the dark-brown spots and necrotic areas caused by the *tig1* mutant were excised, surface sterilized, and incubated on water agar plates for 72 h, we failed to detect fungal growth or conidiation (Figure 2C). Under the same conditions, abundant fungal growth and conidiation were observed over the necrotic areas or lesions caused by Guy11 (Figure 2C). These results indicate that the *tig1* mutant was nonpathogenic and failed to colonize plant tissues through wounds. The rare, small, brown leaf spots caused by the mutant were not true blast lesions and were likely associated with plant defense responses.

To determine whether the *TIG1* function varies among strains, we also generated the *tig1* deletion mutant in strain 70-15 (Chao and Ellingboe, 1991). Mutants KT-2 and KT-4 were identified and confirmed by DNA gel blot analysis to lack *TIG1* (Figure 1B).

These 70-15 *tig1* null mutants displayed the same defects in growth and conidiation as mutant KT-1 (Table 2). On seedlings of rice cultivar Nipponbare, KT-2 and KT-4 failed to cause typical blast lesions in spray or injection infection assays (see Supplemental Figure 2 online).

To confirm that the phenotypes observed in these mutants were directly related to deletion of *TIG1*, mutant KT-4 (*MAT1-1*) was crossed with Guy11 (*MAT1-2*). A total of 19 ascospore progeny were isolated. Eight of these progeny were resistant to hygromycin and had similar defects as the *tig1* mutant. The remaining 11 hygromycin-sensitive progeny had the wild-type phenotype, indicating that defects observed in the *tig1* mutant cosegregated with the hygromycin resistance marker. In addition, we reintroduced the wild-type *TIG1* allele into mutant KT-1. The resulting transformant CT-1 (Table 1) exhibited normal virulence on rice seedlings and produced abundant conidia (Table 2), demonstrating that the inactivation of *TIG1* was responsible for defects of the *tig1* mutant.

TIG1 Is Required for Infectious Growth after Penetration of Rice Cells

When assayed for appressorium formation on artificial hydrophobic surfaces, the *tig1* mutant KT-1 produced abundant melanized appressoria (Figure 3A). No obvious defects in appressorium formation were observed (Table 2). On onion epidermal cells, the mutant exhibited normal levels of appressorium formation. However, it was defective in the penetration of onion epidermal cells and differentiation of invasive hyphae. By 48 h, Guy11

Table 2. Vegetative Growth, Conidiation, and Appressorium Formation in the Wild Type and Transformants Generated in This Study

Strain	Growth Rate on CM (mm/d)	Conidiation ($\times 10^5$ Spores/Plate)	Appressorium Formation (%) ^a
Guy11 (wild type)	6.3 \pm 0.1	280.0 \pm 6.2	99.5 \pm 0.1
KT-1 (<i>tig1</i>)	5.4 \pm 0.2	3.2 \pm 0.7	98.7 \pm 0.2
ECT23 (ectopic)	6.1 \pm 0.2	267.3 \pm 5.6	97.8 \pm 0.2
CT-1 (<i>tig1/TIG1</i>)	6.1 \pm 0.1	289.7 \pm 4.6	95.3 \pm 0.1
70-15 (wild type)	6.2 \pm 0.1	77.5 \pm 2.5	96.7 \pm 0.1
KT-4 (<i>tig1</i>)	5.4 \pm 0.1	0.9 \pm 0.2	90.6 \pm 2.6
KH2-13 (<i>hos2</i>)	4.1 \pm 0.2	0.6 \pm 0.1	92.1 \pm 0.1
KH4-81 (<i>hos4</i>)	5.5 \pm 0.1	7.5 \pm 2.5	94.0 \pm 0.1
KH1-23 (<i>hst1</i>)	6.2 \pm 0.2	26.7 \pm 2.9	93.6 \pm 0.1
ECT1 (ectopic)	6.1 \pm 0.1	49.2 \pm 6.3	96.9 \pm 0.1
Ku80	6.3 \pm 0.1	170.0 \pm 10.0	No data
KS3-1 (<i>set3</i>)	3.4 \pm 0.1	1.7 \pm 0.3	No data
KS1-1 (<i>snt1</i>)	4.1 \pm 0.1	0.4 \pm 0.1	No data
ECT2 (ectopic)	6.3 \pm 0.2	150.0 \pm 12.6	No data

^aPercentage of germ tubes that formed appressoria.

penetrated and formed invasive hyphae inside onion epidermal cells (Figure 3B). Under the same conditions, no invasive hyphae were observed in KT-1. Even up to 72 h, the unbranched primary invasive hyphae formed by KT-1 were blocked in the differentiation and growth of invasive hyphae.

We also assayed appressorium penetration and infectious growth using rice leaf sheath epidermal cells. The *tig1* mutant formed appressoria but failed to develop invasive hyphae in plant cells (Figure 4A). By 48 h, invasive hyphae formed by Guy11 began to invade nearby plant cells. Under the same conditions, unbranched primary invasive hyphae formed by the mutant had only limited growth in penetrated plant cells (Figure 4A). Infected plant cells often had discolored cell walls, and fungal hyphae appeared to be restricted and unhealthy in comparison with those formed by Guy11 (Figure 4A). When stained with 3,3'-diaminobenzidine (DAB), reactive oxygen species (ROS) accumulated around invasive hyphae in plant cells penetrated by the mutant (Figure 4B). By contrast, invasive hyphae formed by Guy11 did not trigger significant ROS accumulation in the host (Figure 4B). These results indicate that the *tig1* deletion mutant is defective in its ability to overcome plant defense responses and maintain biotrophic growth after penetration. When stained with aniline blue, stronger fluorescence signals were observed in barley leaf epidermal cells penetrated by the *tig1* mutant than the wild type (see Supplemental Figure 3 online), suggesting that primary infectious hyphae of the mutant face enhanced callose deposition from the host.

The *tig1* Mutant Has an Increased Sensitivity to H₂O₂ and Plant Defense-Related Proteins

Because plant cells accumulated ROS in the region surrounding primary invasive hyphae of the *tig1* mutant, we tested the sensitivity of the mutant to H₂O₂. When hydrogen peroxide was added to complete medium (CM) plates, fungal growth was decreased with increasing concentrations of H₂O₂. However, the reduction in the growth of the *tig1* mutant was more severe than

that in the wild type. Hyphal growth was completely inhibited by 5 mM H₂O₂ in the *tig1* mutant KT-1 but not in Guy11 (Figure 5A). We also assayed the effects of two plant proteins, osmotin and MsDef1, that are toxic to fungal pathogens (Coca et al., 2000; Ramamoorthy et al., 2007). In the presence of 50 μ g/mL osmotin, appressorium formation was normal in Guy11 but blocked in KT-1 on hydrophobic surfaces (Figure 5B). Osmotin treatment tended to stimulate the formation of multiple germ tubes and unmelanized apical or intercalary swollen bodies. The *tig1* mutant also was more sensitive to MsDef1 than Guy11. In the presence of 20 μ M MsDef1, melanized appressoria were formed by Guy11 but not by KT-1 (Figure 5B). Unlike osmotin, MsDef1 treatment did not cause KT-1 germ tubes to swell.

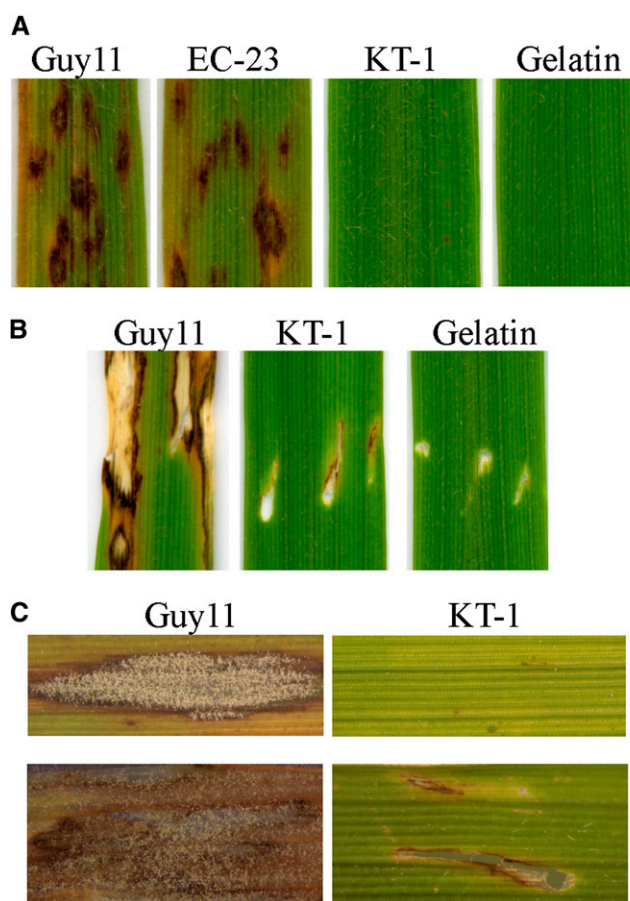


Figure 2. Infection Assays with the *tig1* Mutant.

(A) Rice leaves sprayed with conidia from the wild-type strain Guy11, an ectopic transformant ECT23, and *tig1* mutant KT-1.

(B) Injection assays with Guy11 and KT-1. Inoculation with 0.25% gelatin was the negative control. The *tig1* mutant only caused limited necrosis at the wound site.

(C) Assays for fungal growth on surface-sterilized rice leaves inoculated by spray (top panels) or injection (bottom panels). Abundant hyphae and conidia were observed on leaves inoculated with Guy11. No fungal growth was observed on rare brown spots or limited necrotic regions at the wound sites caused by the *tig1* mutant.

[See online article for color version of this figure.]

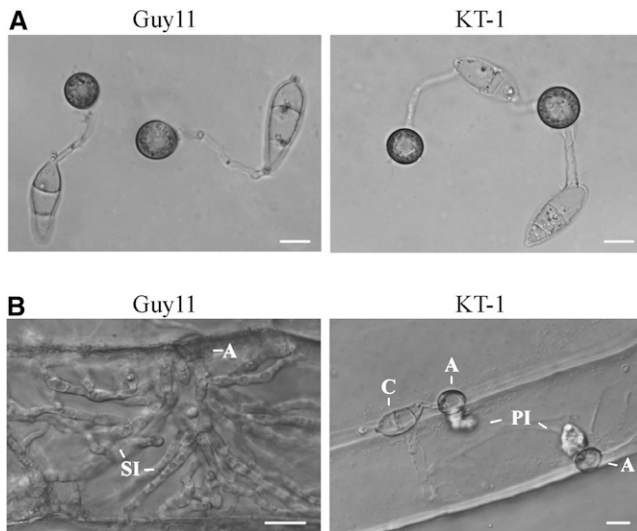


Figure 3. Appressoria Formation and Penetration of Onion Epidermal Cells.

(A) Melanzized appressoria formed by the wild type (Guy11) and *tig1* mutant (KT-1) strains on plastic cover slips.

(B) Penetration assays with onion epidermal cells. By 48 h, invasive hyphae were observed in plant cells penetrated by Guy11 but not KT-1. A, appressorium; C, conidium; PI, primary invasive hyphae; SI, secondary invasive hyphae.

Bars = 10 μ m.

Identification of *TIG1*-Interacting Proteins by Affinity Purification

TIG1 is putatively orthologous to yeast *SIF2*, which is a member of the Set3 complex involved in the late stages of ascospore formation (Pijnappel et al., 2001; Cerna and Wilson, 2005). To determine whether *TIG1* functions in a similar complex in *M. oryzae*, we generated a *TIG1*-3xFLAG construct and transformed it into 70-15. In transformant TFg1 (Table 1), a 72-kD band of the expected size of Tig1-3xFLAG was detected with an anti-FLAG antibody in proteins isolated from vegetative hyphae grown in liquid CM medium (see Supplemental Figure 4 online).

For affinity purification, total proteins were isolated from transformant TFg1 and mixed with anti-FLAG M2 beads. Proteins bound to M2 beads were eluted and digested with trypsin and identified by mass spectrometry analysis (see Methods). Table 3 lists proteins that were copurified with the *TIG1*-3xFLAG fusion. MGG_09174.5, MGG_01663.5, MGG_02488.5, MGG_10447.5, and MGG_05727.5 (Table 3) are orthologous to yeast *SNT1*, *HOS2*, *HST1*, *CPR1*, and *HOS4*, respectively, which are members of the Set3 complex (Pijnappel et al., 2001; Mou et al., 2006). They were consistently identified as *TIG1*-interacting genes in four independent biological replicates. Other proteins that coimmunoprecipitated with Tig1 included MGG_09602.5 and MGG_01362.5 (Table 3). While MGG_09602.5 has no homologous sequence in *Saccharomyces cerevisiae* and appears to be unique to filamentous fungi, putative orthologs of other genes exist in yeast. MGG_01362.5 is homologous to yeast Cdc28,

which interacts with Hos4 (Ubersax et al., 2003), but does not belong to the Set3 complex.

TIG1 Is a Member of a Conserved HDAC Protein Complex

The putative orthologs of all members of the yeast Set3 complex except Set3 itself copurified with Tig1 (Table 3). We amplified the predicted open reading frame (ORF) of MGG_01558 (named *SET3* in this study) and cloned it into the pAD-GAL4 prey vector. The *TIG1* gene was cloned into the corresponding bait vector. Growth on SD-His plates and LacZ activity were detected in yeast cells expressing the *SET3* prey and *TIG1* bait constructs (Figure 6A), indicating that *SET3* interacted with *TIG1*. However, their interaction was relatively weak in comparison with the positive control for yeast two-hybrid assays (Figure 6A).

To confirm the *TIG1*-*SET3* interaction, we generated the *SET3*-green fluorescent protein (GFP) construct and cotransformed it into 70-15 with the *TIG1*-3xFLAG fusion. The resulting hygromycin-resistant transformant TS-29 (Table 1) was confirmed by PCR to contain both constructs, and successful transformation was further confirmed by immunoblot analysis with anti-FLAG and anti-GFP antibodies. Total proteins were isolated from transformant TS-29 and bound to anti-FLAG M2 beads. Proteins bound to the bead were eluted, separated on 12% SDS-PAGE gels, and transferred onto nitrocellulose membrane. As expected, the Tig1-3xFLAG protein was detected with an anti-FLAG antibody in both the eluted and total proteins (Figure 6B). A protein band of the expected size of the Set3-GFP fusion was also detected with the anti-GFP antibody in both the elution and total proteins (Figure 6B), indicating that Set3 coimmunoprecipitated with Tig1. The anti-actin antibody detected the actin band in total proteins isolated from the transformant, but not in the eluted proteins (Figure 6B).

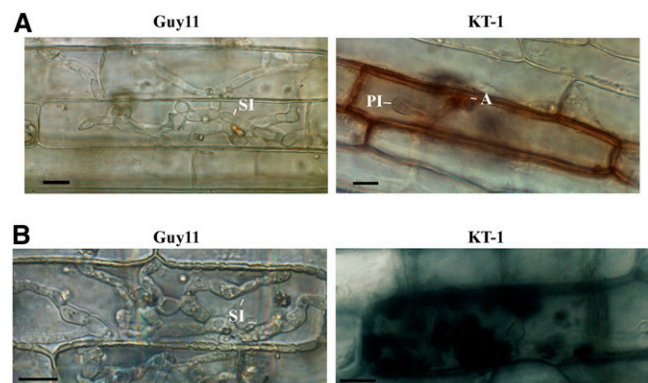


Figure 4. Penetration Assays with Rice Leaf Sheath Epidermal Cells.

(A) Extensive invasive hyphae were developed by Guy11 inside plant cells by 72 h after inoculation. The *tig1* mutant (KT-1) had only limited growth of primary invasive hyphae.

(B) When stained with DAB, rice cells penetrated by the *tig1* mutant accumulated ROS around fungal hyphae. No obvious ROS accumulation was observed in plant cells penetrated by Guy11. A, appressorium; PI, primary invasive hyphae; SI, secondary invasive hyphae.

Bars = 10 μ m.

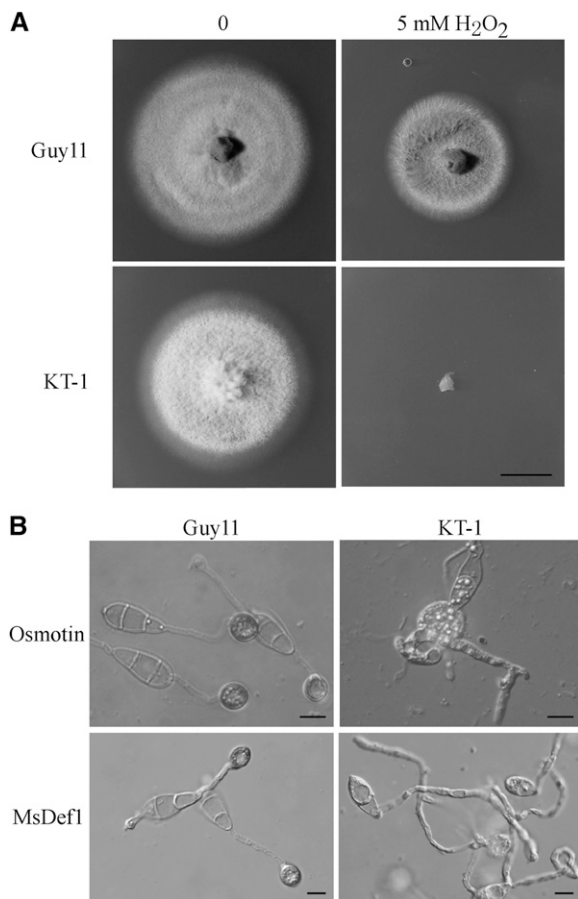


Figure 5. Increased Sensitivities of the *tig1* Mutant to Hydrogen Peroxide, Osmotin, and MsDef1.

(A) CM cultures of the wild-type (Guy11) and *tig1* mutant (KT-1) strains in the presence or absence of 5 mM H₂O₂. Bar = 1 cm.

(B) In the presence of 50 μg/mL osmotin (top panels) or 20 μM MsDef1 (bottom panels), melanized appressoria were formed by Guy11 but not KT-1 by 24 h after inoculation. Osmotin treatment resulted in the formation of multiple germ tubes and apical or intercalary swollen bodies in the *tig1* mutant. Bars = 10 μm.

Similarly, coimmunoprecipitation (co-IP) assays were conducted to confirm the interactions between *SET3* and *HOS2* (Figure 7A) and *TIG1* and *HOS2* (Figure 7B) in *M. oryzae*. We generated the *SET3*-3xFLAG and *HOS2*-GFP constructs and transformed them into strain 70-15 in pairs or individually with the *TIG1* fusion construct. Transformants HT-26 and HS-9 (Table 1), expressing the *TIG1*-3xFLAG/*HOS2*-GFP and *SET3*-3xFLAG/*HOS2*-GFP fusion constructs, respectively, were identified. The same GFP fusion band was detected in both the total proteins isolated from vegetative hyphae and proteins eluted from anti-FLAG M2 beads in both HT-26 (Figure 7A) and HS-9 (Figure 7B). These data indicate that Hos2 interacts with Set3 and Tig1 in vivo. The results of these co-IP assays suggest that Tig1 belongs to a *M. oryzae* protein complex that is similar to the yeast Set3 complex.

SNT1, *HOS2*, and *SET3* Are Required for Plant Infection

To determine the functions of Tig1-interacting proteins, we constructed deletion mutants of *SNT1*, *HOS2*, *SET3*, *HST1*, and *HOS4* by gene replacement. The putative *CPR1* ortholog, *CYP1*, was not included in this study because it is known to be involved in plant infection in *M. oryzae* (Viaud et al., 2002). The *snt1*, *set3*, *hos4*, *hos2*, and *hst1* deletion mutants (Table 1) were identified by PCR and confirmed by DNA gel blot analysis (see Supplemental Figure 5 online). Like the *tig1* mutant, *snt1*, *set3*, and *hos2* mutants were nonpathogenic on seedlings of susceptible rice cultivars (Figure 8A) and barley (Figure 8B). These three mutants were also greatly impaired in conidiation (Table 2). By contrast, conidiation was not significantly impaired in the *hst1* and *hos4* mutants (Table 1), and these mutants were as virulent as the wild type (Figures 8A and 8B), indicating that *HST1* and *HOS4* are dispensable for plant infection and the function of the Tig1 complex.

In addition to reduced conidiation, conidia formed by the *tig1*, *snt1*, *set3*, and *hos2* mutants varied significantly in size and morphology from those formed by the wild type (Figure 8C). In general, conidia from these mutants were still three celled, but most of them were narrower than wild-type conidia. Some conidia produced by the *tig1*, *snt1*, *set3*, and *hos2* mutants no longer had the normal pyriform shape (Figure 8C). A reduction in conidiation and abnormal spore morphology indicate that *TIG1*, *SNT1*, *SET3*, and *HOS2* play an important role in conidiogenesis in *M. oryzae*. We performed a complementation analysis, in which wild-type *HOS2* and *SET3* genes were reintroduced into the *hos2* and *set3* mutants, respectively. The resulting complemented transformants (CH-1 and CS-1; Table 1) exhibited normal virulence (Figure 8B), conidiation, and conidium morphology.

HDAC Activities and Histone Acetylation in the Tig1 Complex Mutants

Because the yeast Set3 complex is involved in histone deacetylation, it is likely that Tig1, Set3, Hos2, and Snt1 are components of a similar HDAC complex in *M. oryzae*. Therefore, we assayed HDAC activities in protein extracts isolated from protoplasts of the *tig1*, *set3*, *hos2*, and *snt1* mutants. In comparison with the wild-type strains, the *tig1*, *set3*, *snt1*, and *hos2* mutants were highly reduced in HDAC activities (Figure 9A). The three wild-type

Table 3. Putative TIG1-Interacting Genes Identified by Affinity Purification

Gene ID	Yeast Homolog
MGG_01633.5	<i>HOS2</i>
MGG_09174.5	<i>SNT1</i>
MGG_02488.5	<i>HST1</i>
MGG_10447.5	<i>CPR1</i>
MGG_05727.5	YIL112w (<i>HOS4</i>)
MGG_06453.5	YCR028C
MGG_09602.5	No homolog
MGG_00446.5	YGL019W (CKB1)
MGG_01826.5	YGL174W (BUD13)
MGG_01362.5	YBR160W (CDC28)
MGG_03741.5	YGR266W

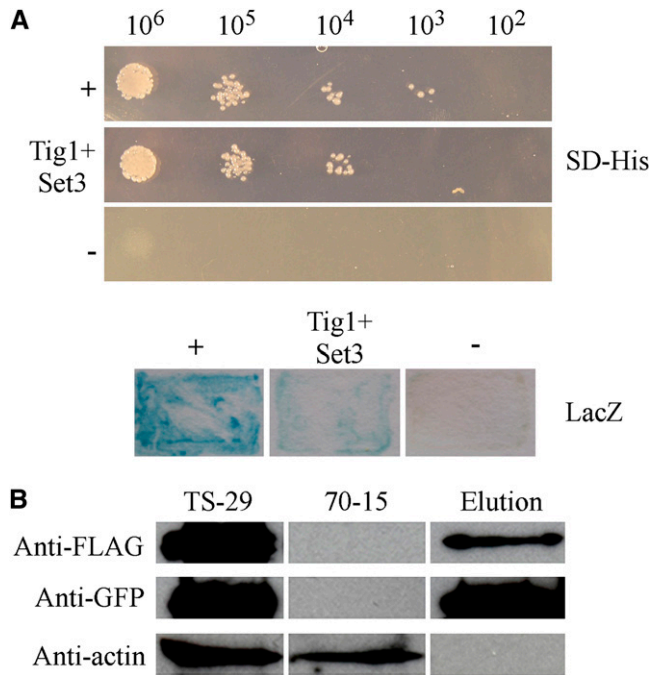


Figure 6. Yeast Two-Hybrid and Coimmunoprecipitation Assays for the *TIG1-SET3* Interaction.

(A) Yeast transformants expressing the *TIG1* bait and *SET3* prey constructs were assayed for growth on SD-Leu-Trp-His plates (SD-His) and β -galactosidase (LacZ) activities. +, Positive control; -, negative control. **(B)** Immunoblot analysis of total proteins (TS-29) and proteins eluted from the anti-FLAG M2 beads (Elution) of transformant TS-29 that expressed the *TIG1*-3xFLAG and *SET3*-GFP constructs. Total proteins isolated from the wild-type strain (70-15) were included as the control. Top, middle, and bottom images represent detection with anti-FLAG, anti-GFP, and anti-actin antibodies, respectively. [See online article for color version of this figure.]

strains, Guy11, 70-15, and Ku80, used for generating these mutants had similar HDAC activities in three biological replicates (Figure 9A). These results indicate that Tig1, Set3, Hos2, and Snt1 are required for the activity of the HDAC complex in *M. oryzae*. Because *TIG1*, *SET3*, and *SNT1* have no predicted functions in histone modification, their effects on histone acetylation must be related to their participation in an HDAC complex.

Since reduced HDAC activities may lead to increased histone acetylation, we assayed the acetylation level of histone H3 in the *hos2* mutant. In nuclear proteins isolated from Guy11, the expression level of histone 3 was similar to that of the mutant. However, when detected with an anti-H3K18Ac antibody that is specific for K18 acetylation of histone H3 (Figure 9B), Guy11 had weaker signals than the *hos2* mutant, indicating that the *hos2* mutant had higher levels of H3K18 acetylation than Guy11.

Disruption of the Tig1 Complex Affects the Activation of Mps1 MAP Kinase

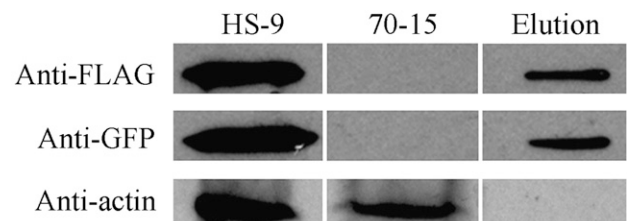
Since the Set3 complex functions upstream of the Sit2 MAP kinase during secretory stress responses (Cohen et al., 2008), we

assayed the activation of Mps1 in the mutants disrupted in the Tig1 complex. In vegetative hyphae, the expression of Mps1 was not affected by *SNT1*, *TIG1*, or *SET3* deletion (Figure 9C). However, the phosphorylation level of Mps1 was lower in the *snt1*, *tig1*, and *set3* mutants than in Ku80 (Figure 9C), indicating a reduction in Mps1 activation in these mutants disrupted in the Tig1 complex. By contrast, phosphorylation of Pmk1 was not affected or was slightly increased in the *snt1*, *tig1*, and *set3* mutants (Figure 9C).

Expression and Localization of *TIG1*-, *SET3*-, and *HOS2*-GFP

Although Tig1 has no predictable nuclear localization signal (NLS) sequences, it may localize to the nucleus as one component of a HDAC complex. To test this hypothesis, a *TIG1*-GFP fusion construct was transformed into the *tig1* mutant KT-1. Transformant KT1NG1 (Table 1), which expresses the *TIG1*-GFP fusion, exhibited normal growth, conidiation, and virulence, indicating that the defects in the *tig1* mutant were complemented. In KT1NG1, GFP signal was observed in the nucleus in conidia, appressoria, and invasive hyphae (Figure 10A). In vegetative hyphae, only a faint GFP signal was observed in the nuclei of some hyphal compartments (Figure 10A). When the *TIG1*-GFP fusion was overexpressed with the RP27 promoter in transformant KT1RP1 (Table 1), a stronger GFP signal was observed in the nuclei of vegetative hyphae (see Supplemental Figure 6 online), suggesting that lower expression of *TIG1*-GFP was responsible for weak GFP signals in vegetative hyphae in KT1NG1.

A Set3 - Hos2



B Tig1 - Hos2

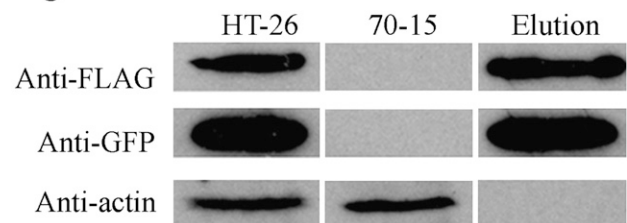


Figure 7. Co-IP Assays for Interactions between Components of the Tig1 Complex.

Co-IP assays of transformants HS-9 **(A)** and HT-26 **(B)** that expressed the *SET3*-FLAG/*HOS2*-GFP and *TIG1*-3xFLAG/*HOS2*-GFP constructs, respectively. Immunoblots of total proteins isolated from each transformant and proteins eluted from the anti-FLAG M2 beads (Elution) were detected with the anti-FLAG, anti-GFP, or anti-actin antibody. Total proteins isolated from the wild-type strain 70-15 were included as the control.

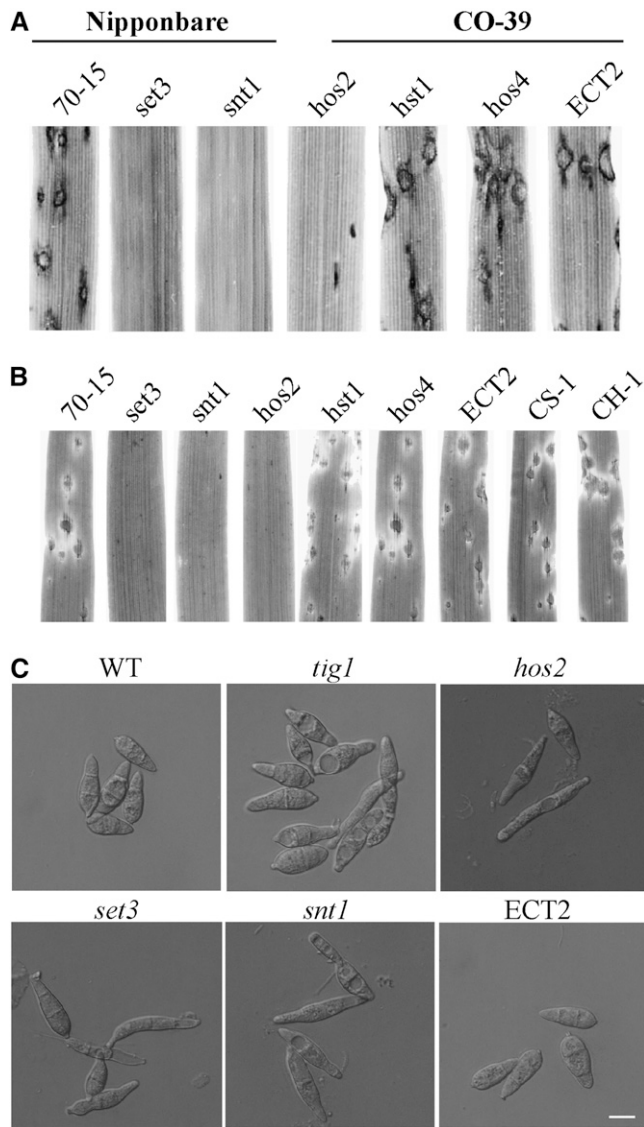


Figure 8. Pathogenicity and Conidium Morphology of Mutants Disrupted in the *TIG1* Complex.

(A) Leaves of rice cultivar Nipponbare or CO-39 were inoculated with conidia from 70-15, the *set3*, *snt1*, *hos2*, *hst1*, and *hos4* mutants, and an ectopic transformant of Ku80 (ECT2).

(B) Barley leaves sprayed with the same set of strains described above. The *hst1* and *hos4* mutant had normal virulence, but the *set3*, *snt1*, and *hos2* mutants were nonpathogenic. CH-1 and CS-1 were complemented transformants of the *hos2* and *set3* null mutant, respectively.

(C) Conidia of 70-15, *tig1* and *set3* mutants, and ectopic transformant ECT2. Bar = 10 μ m.

We also generated GFP fusion constructs with *SET3* and *HOS2*. In transformants of 70-15 expressing these constructs (Table 1), the GFP signal was also observed in the nucleus in conidia, appressoria, and invasive hyphae (Figure 10B). Similar to the *TIG1*-GFP transformant, the expression of *SET3*-GFP was

lower in vegetative hyphae than invasive hyphae, but a faint GFP signal could be observed in some nuclei. However, in transformants expressing the *HOS2*-GFP fusion, GFP signals were weak or not detectable in vegetative hyphae.

Expression Profiles of Selected Components of the Tig1 Complex

We used quantitative RT-PCR (qRT-PCR) to quantify the transcripts of *TIG1*, *HOS2*, *HOS4*, *HST1*, *SET3*, and *SNT1* at different fungal developmental and infection stages. All of these genes were expressed at a relatively low level in vegetative hyphae and had their highest expression levels in conidia (Figure 11). In comparison with their expression levels in vegetative hyphae, transcription of *TIG1*, *HOS2*, *HOS4*, *HST1*, *SET3*, and *SNT1*

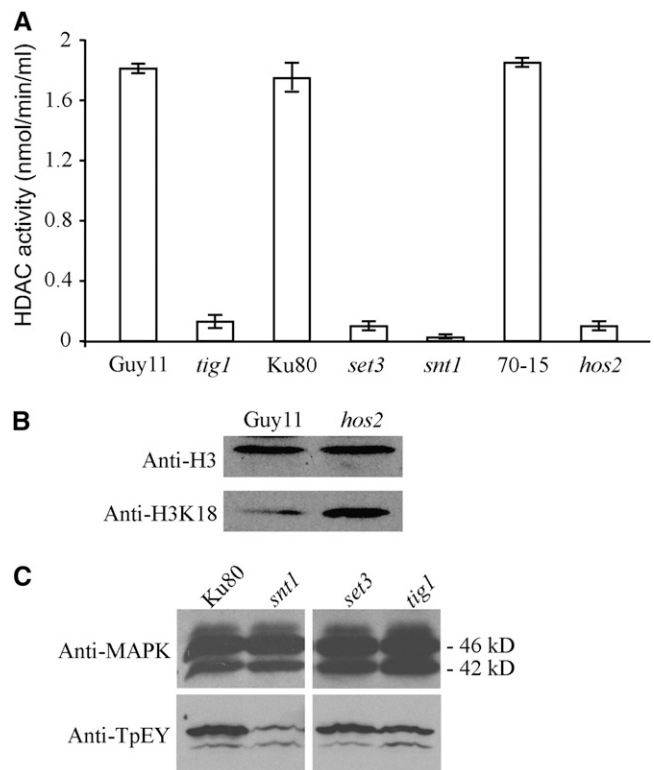


Figure 9. Assays for HDAC Activity and Histone H3 Acetylation in *M. oryzae* Strains.

(A) HDAC activities were assayed with proteins isolated from the wild-type strains Guy11, 70-15, and Ku80 and from the *tig1* (KT-1), *set3* (KS3-1), *snt1* (KS1-1), and *hos2* (KH2-13) mutants. Median and SD were calculated from three biological replicates.

(B) Immunoblots of nuclear proteins isolated from Guy11 (wild type) and the *hos2* mutant were detected with the anti-histone 3 antibody (anti-H3; top panel) or the anti-H3K18Ac antibody (anti-H3K18; bottom panel). The level of H3K18 acetylation was higher in the mutant than in Guy11.

(C) Immunoblots of total proteins from Ku80 and the *set3*, *snt1*, and *tig1* mutants were detected with an anti-MAPK antibody (top panel) and an anti-TpEY antibody (bottom panel). Both the Mps1 (46-kD) and Pmk1 (42-kD) MAP kinases could be detected.

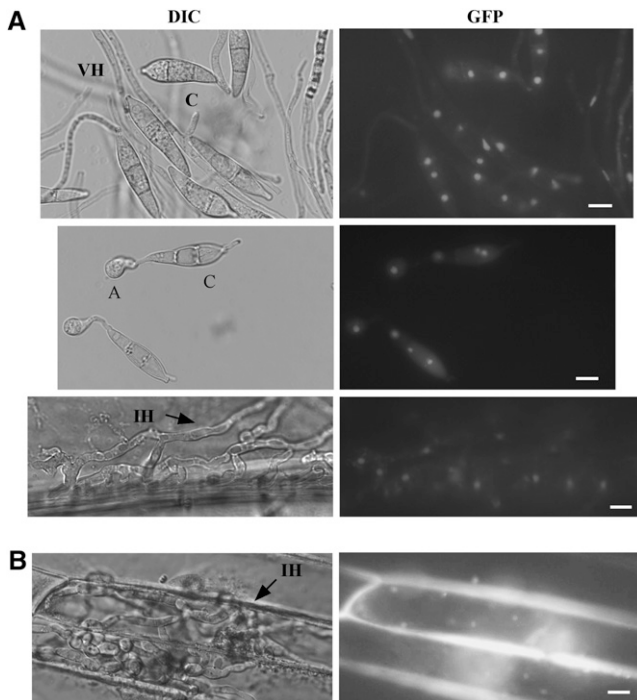


Figure 10. Expression and Localization of the GFP Fusion Proteins.

(A) In transformant KT1NG1, which expresses the *TIG1*-GFP fusion, GFP signals were observed in the nucleus in conidia (top), appressoria (middle), and invasive hyphae (bottom). A, appressoria; C, conidia; VH, vegetative hyphae; IH, invasive hyphae.

(B) Nuclear localization was also observed in the invasive hyphae of transformant CS-1, which expresses the *SET3*-GFP fusion.

Bars = 10 μ m.

increased 23-, 6-, 25-, 46-, 16-, and 27-fold, respectively, in conidia. These results were in agreement with the weaker GFP signal observed in vegetative hyphae than in conidia in transformants expressing the *TIG1*-GFP or *HOS2*-GFP fusion.

The expression of *TIG1*, *HOS2*, *HOS4*, *HST1*, *SET3*, and *SNT1* was higher in appressoria than in vegetative hyphae (5- to 13-fold; Figure 11), but they all had the highest expression level in conidia (Figure 11). Transcripts of these six genes were not detectable by qRT-PCR during the early stages of infection (1 to 2 d after inoculation [DAI]), likely as a consequence of a combination of their low expression levels (<0.1-fold of the reference gene *ILV5* encoding an acetohydroxyacid reductoisomerase) and a low percentage of fungal RNA in these infected rice leaves (<1% of total RNA). Among all of the genes assayed by qRT-PCR, only the expression of *CYP1* was detectable during the early infection stages (1 to 2 DAI; see Supplemental Figure 7 online), which is likely related to its expression level being 2- to 4-fold higher than that of the reference gene *ILV5*. At later infection stages (3 to 4 DAI), transcripts of all of these genes were detectable by qRT-PCR. At 4 DAI, the expression level of *TIG1*, *HOS2*, *HOS4*, *HST1*, *SET3*, and *SNT1* was 4-, 3-, 5-, 6-, 4-, and 6-fold higher in infected leaves than in vegetative hyphae, respectively (Figure 11). These data indicate that all of the proposed components of the Tig1 complex, except for *CYP1*,

share the same expression pattern at the different fungal developmental and infection stages.

DISCUSSION

In this study, we identified and characterized the *TIG1* gene and protein complex in *M. oryzae*. *TIG1* and its orthologs are conserved from yeast to human (Pijnappel et al., 2001; Mou et al., 2006). *TIG1* shares higher similarity with mammalian *TBL1* than with yeast *SIF2*. It has an N-terminal LisH domain and six WD domains in the C-terminal region. No other genes in *M. oryzae* have similar structural features. We also noticed that many of the *TIG1* orthologs from filamentous fungi have an intron in the LisH domain and another intron immediately before the stop codon. These two introns at the termini of *TIG1* ORF may be evolutionarily conserved for regulating the expression or stability of *TIG1* mRNA.

In budding yeast, Sif2 is involved in transcriptional repression of meiosis-specific genes (Pijnappel et al., 2001; Cerna and Wilson, 2005). In *M. oryzae*, the *tig1* mutant was female sterile but male fertile. Among 30 ascospore progeny from a *tig1* \times *TIG1* cross, 18 carried the *tig1* null allele, suggesting that *TIG1* deletion has no effect on ascospore formation and viability. However, conidiation was significantly reduced in the *tig1* and other Tig1 complex-deficient mutants (Table 2). Conidium morphology was also abnormal in these mutants (Figure 8C). Because asexual reproduction plays a critical role in the infection cycle, the Tig1 complex may have been adapted to regulate conidiation in *M. oryzae* and other plant pathogens. In a number of phytopathogenic fungi, MAP kinases involved in the yeast pheromone response and filamentous growth pathways have evolved to regulate appressorium formation and other plant infection processes (Zhao et al., 2007; Rispaill et al., 2009).

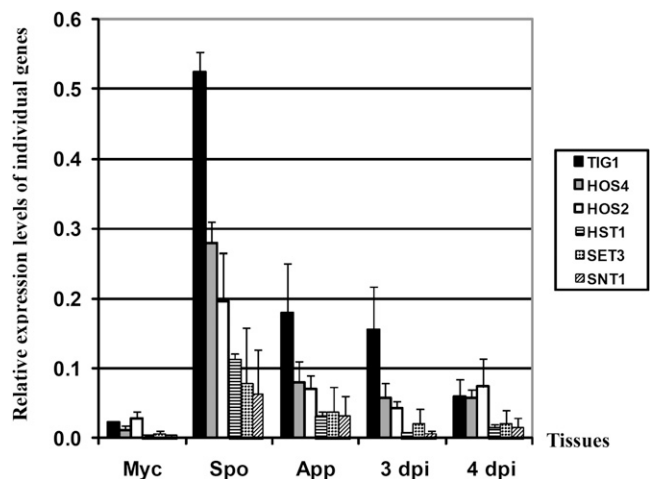


Figure 11. Expression Patterns of Genes Associated with *TIG1*.

Expression levels of *TIG1*, *HOS2*, *SNT1*, *HOS4*, *SET3*, and *HST1* in vegetative hyphae (Myc), conidia (Spo), 24-h-old appressoria (App), and infected rice leaves harvested at 3 or 4 DAI. qRT-PCR was used to quantify transcripts of these genes relative to that of the constitutive reference gene *ILV5* using the $2^{-\Delta\Delta C_T}$ method. Median and SD were calculated from three biological replicates.

Similar to *ftl1* mutants in *F. graminearum* (Ding et al., 2009), the *tig1* mutant was nonpathogenic. Close examination indicates that the differentiation of invasive hyphae was blocked in the *tig1* mutant. In plant cells penetrated by the *tig1* mutant, only limited growth of primary invasive hyphae was observed. DAB staining indicated that *tig1* primary invasive hyphae were surrounded by a high concentration of ROS. Plant cells appeared to mount strong defense responses and displayed HR-like cell death. The *tig1* mutant also had increased sensitivities to PR protein osmotin and plant defensin MsDef1 (Coca et al., 2000; Ramamoorthy et al., 2007). It is possible that attenuated invasive growth of the *tig1* mutant triggered strong defense responses in host cells. Rapid accumulation of high concentrations of ROS and other plant defense compounds at the penetration site may block the proliferation of the *tig1* mutant and subsequently result in the death of penetrated plant cells, which may be responsible for the rare, small brown spots formed on susceptible rice seedlings inoculated with the *tig1* mutant (Figure 2A).

In comparison with extensive studies on appressorium formation and function, the regulation of postpenetration infection processes is not well characterized in *M. oryzae* (Ebbole, 2007; Xu et al., 2007; Wilson and Talbot, 2009). Unlike other nonpathogenic mutants that are blocked in either appressorium formation or appressorium-mediated penetration, mutants disrupted in the Tig1 HDAC complex were defective in the differentiation and growth of bulbous secondary invasive hyphae. These results indicate that chromatin modification plays a critical role in regulating fungal invasive growth. Because histone deacetylation is normally associated with a suppression of gene expression (Pijnappel et al., 2001; Brosch et al., 2008), the Tig1 complex may be involved in the repression of genes that are detrimental to the differentiation and biotrophic growth of secondary invasive hyphae. The fact that *M. oryzae* uses a global regulatory mechanism such as histone modification for invasive growth indicates that a large number of genes may need to be repressed simultaneously in invasive hyphae. Further characterization of the Tig1 complex will be helpful in understanding the regulatory networks that regulate fungal-plant interactions after penetration and development of invasive hyphae.

In mammalian cells, *TBL1* and *TBLR1* are transducin β -like proteins associated with the N-CoR (nuclear receptor corepressor) and SMRT (silencing mediator for retinoid and thyroid hormone receptors) complex (Guenther et al., 2001; Yoon et al., 2003; Zhang et al., 2006). SMRT proteins have an N-terminal domain that binds to nuclear receptors and a C-terminal region that interacts with HDACs. In yeast, Sif2 is a component of the Set3 HDAC complex that consists of Sif2, Hos2, Set3, Snt1, Hst1, Hos4, and Cpr1 (Pijnappel et al., 2001; Cerna and Wilson, 2005; Mou et al., 2006). Several of these proteins are conserved from yeast to human. The *M. oryzae* genome contains putative orthologs of every component of the yeast Set3 complex. All of these putative orthologs except *SET3* were coimmunoprecipitated with the Tig1-3xFLAG fusion. However, only a weak interaction was detectable between Tig1 and Set3 in yeast two-hybrid assays. The Tig1-Set3 interaction was further confirmed by co-IP assays. We also confirmed the Tig1-Hos2 and Set3-Hos2 interactions by co-IP. *SNT1* was not included in the co-IP assays because of its size (~8 kb) and the difficulty of making fusion constructs.

Overall, our results suggest that Tig1 functions in a protein complex that is similar to the yeast Set3 complex. The Tig1 complex of *M. oryzae* likely contains Tig1, Set3, Hos2, Snt1, Hst1, Hos4, and Cyp1.

Similar to the *tig1* mutant, the *set3*, *hos2*, and *snt1* mutants had altered conidium morphology and were defective in plant infection. By contrast, the *hst1* and *hos4* mutants had no obvious defects in conidiogenesis and pathogenesis. These results indicate that *TIG1*, *SET3*, *HOS2*, and *SNT1*, but not *HST1* and *HOS4*, are involved in regulating similar biological processes in *M. oryzae*. In yeast, *SIF2*, *SET3*, *HOS2*, and *SNT1* are core components of the Set3 complex. Our results indicate that essential components of the *M. oryzae* Tig1 complex are Tig1, Set3, Hos2, and Snt1. Deletion of any one of these components may disrupt the integrity and function of this Tig1 complex. The putative Cpr1 ortholog, *CYP1*, is known to be involved in calcium signaling and to be required for virulence in *M. oryzae* (Viaud et al., 2002).

Based on the similarities in composition, the Tig1 complex appeared to function as a Set3-like HDAC complex in *M. oryzae*. The HDAC activities in the *tig1*, *set3*, *hos2*, and *snt1* mutants were significantly reduced in comparison with that of the wild type. HDACs catalyze the removal of acetyl groups from Lys residues in histones and nonhistone proteins (Ficner, 2009). The *tig1*, *set3*, *hos2*, and *snt1* mutants had increased levels of H3K18 acetylation. Further indirect evidence that these proteins are essential components of a Set3-like HDAC complex is that Tig1-, Set3-, and Hos2-GFP fusion proteins all localized to the nucleus. Tig1 has no predictable NLS sequence. Its association with other components of the complex may be responsible for nuclear localization of the Tig1-GFP fusion proteins. Unlike Tig1, the Set3 and Snt1 proteins have putative NLS sequences.

Recently, the core components of the Set3 complex, including Hos2, Set3, Sif2, and Snt1, have been shown to be important for efficient responses to secretory stress via the Slt2 MAP kinase pathway in yeast (Cohen et al., 2008). In *M. oryzae*, *MPS1* and *BCK1*, putative orthologs of yeast Slt2 and Bck1, are important for fungal cell wall integrity and pathogenesis (Xu et al., 1998; Jeon et al., 2008). In this study, we showed that phosphorylation of Mps1 was reduced in the *tig1*, *set3*, and *snt1* mutants (Figure 9). Similar to the *mpe1* mutant (Xu et al., 1998), conidiation was significantly reduced in the *tig1* mutant. It is likely that the Tig1 HDAC complex plays a role in the activation of the Mps1 pathway in response to certain stresses or signals in *M. oryzae*.

As a key component of the Tig1 complex, *HOS2* had increased expression levels in conidia, appressoria, and infected rice leaves at 3 to 4 DAI (Figure 11), and expression was highest in conidia. This expression pattern is shared by all the genes encoding components of the Tig1 HDAC complex, except for *CYP1* (see Supplemental Table 5 online). *HOS2* is a class II HDAC gene. In yeast, *HDA1* and *HOS3* are two other class II HDAC genes (Trojer et al., 2003), but they are not part of the Set3 complex. The *M. oryzae* genome contains HDAC genes that are putatively orthologous to yeast *HDA1* and *HOS3*. While the expression of *HDA1* (MGG_01076.5) was higher in appressoria than in conidia, *HOS3* (MGG_06043.5) had an expression pattern similar to that of *HOS2* in vegetative hyphae, conidia, and appressoria (see Supplemental Figure 7 online). Deletion of *HDA1* and *HOS3* had no obvious effects on fungal growth,

conidiogenesis, and appressorium formation. Unlike the *hos2* mutant, *hda1* and *hos3* null mutants were still pathogenic on rice and barley leaves (see Supplemental Figure 8 online). While the *hda1* mutant was delayed in symptom development for about 1 d, the *hos3* mutant had slightly reduced virulence. These results suggest that Hos2 is the main class II HDAC in *M. oryzae*.

TIG1-interacting genes, including *SET3*, *SNT1*, and *HOS2*, are also conserved in the genomes of other filamentous fungi that have been sequenced. However, none of the putative *SET3* and *SNT1* orthologs had previously been functionally characterized in plant pathogenic fungi. For *HOS2*, its putative ortholog in *Cochliobolus heterostrophus* is an important pathogenicity factor, but its role in conidiogenesis is not clear (Baidyaroy et al., 2001). In *F. graminearum*, we also generated mutants that lack the putative orthologs of yeast *SET3*, *HOS2*, and *SNT1*. Similar to the *ftl1* mutant, the *Fgset3*, *Fghos2*, and *Fgsnt1* mutants were defective in plant infection and conidiogenesis (J.-R. Xu, unpublished data), indicating that the Tig1-HDAC complex plays a similar role in *M. oryzae* and *F. graminearum*, and possibly also in other fungal pathogens, by regulating genes important for pathogenesis and conidiogenesis. To date, the molecular mechanisms that regulate the expression of genes that are specifically expressed or highly induced in invasive hyphae, such as *BAS* or other effector genes (Mosquera et al., 2009), are not clear in *M. oryzae*. Our results indicate that the Tig1 HDAC complex regulates the differentiation and growth of secondary invasive hyphae after penetration. The identification and characterization of downstream target genes of this well-conserved HDAC complex will enhance our understanding of the regulatory networks that regulate gene expression in invasive hyphae or during the early stages of plant colonization.

METHODS

Culture Conditions and Genetic Manipulations

All the wild-type and mutant strains used in this study (Table 1) were cultured on oatmeal agar or CM plates as described (Talbot et al., 1993; Park et al., 2006; Villalba et al., 2008). Mycelia harvested from 2-d-old 5×YEG (0.5% yeast extract and 1% glucose) cultures shaken at 150 rpm were used for isolation of genomic DNA and protoplasts (Sweigard et al., 1998; Zhao et al., 2005). Hygromycin- or zeocin-resistant transformants were selected on media supplemented with 250 μg/mL hygromycin B or 150 μg/mL zeocin (Invitrogen). Protoplast transformation and genetic crosses were performed as described previously (Talbot et al., 1993; Zhao and Xu, 2007).

Appressorium Formation and Plant Infection Assays

Conidia harvested from 10-d-old oatmeal agar cultures were resuspended to 1×10^4 spores/mL in water for appressorium formation and penetration assays and to 1×10^9 spores/mL in 0.25% gelatin for plant infection assays (Li et al., 2007; Mosquera et al., 2009). Two-week-old seedlings of rice (*Oryza sativa*) cultivar CO-39, Nipponbare, or Sariceltik and 8-d-old seedlings of barley (*Hordeum vulgare*) cultivar Golden Promise or Plaisant were used for infection assays (Park et al., 2004). To isolate *Magnaporthe oryzae* from infected leaves, wound inoculation sites and areas of typical blast lesions or brown spots were excised, surface sterilized, and incubated on 2% water agar as described (Xu and Hamer, 1996). Fungal growth and conidiation were observed after incubation for 2 to 3 d. For

staining with DAB (Sigma-Aldrich), rice leaf sheath samples were incubated in 1 mg/mL DAB solution, pH 3.8, for 8 h and destained with ethanol/acetic acid (94/4, v/v) for 1 h before examination. For aniline blue staining (Bhambra et al., 2006), barley leaves were sampled 72 h after inoculation and incubated in 1 M KOH at 70°C for 20 min. After washing three times with water and once with 67 mM K₂HPO₄, pH 9.0, the samples were stained with 0.05% aniline blue and examined with a Nikon epifluorescence microscope. For RNA isolation, infected leaves of cultivar Sariceltik were sampled at 1, 2, 3, and 4 DAI. Osmotin (Coca et al., 2000) and MsDef1 (Ramamoorthy et al., 2007) were added to conidium suspensions to final concentrations of 20 and 50 μM, respectively for assaying their effects on germination and appressorium formation.

Manual Annotation of *TIG1* and *SNT1*

Sequencing analysis of *TIG1* cDNA clones showed that the ORF of MGG_03198 was incorrectly predicted in version 6 of the *M. oryzae* genome annotation (incorrect start codon and first two introns). MGG_03198.5 (version 5) was similar to the cDNA sequence. The *SNT1* gene also differs in version 5 (MGG_09174.5) and version 6 (MGG_14558.6 and MGG_14559.6). Other genes described in this article are similar in versions 5 and 6 of the genome annotation.

Molecular Manipulations

RNA was isolated from mycelia or infected rice leaves (Vergne et al., 2007) with TRIzol reagent (Invitrogen) and purified with the DNA-free kit (Ambion). First-strand cDNA was synthesized with the M-MLV reverse transcriptase (Invitrogen). qRT-PCR was performed with the ABI 7700 sequence detection system (Applied Biosystem) using QuantiTect SYBR-green PCR Master Mix (Qiagen) as described (Flaherty and Dunkle, 2005). Primers used to amplify selected genes in qRT-PCR reactions are listed in Supplemental Table 1 online. *ACT1* (Li et al., 2007), *TUB1* (MGG_00604.5), or *ILV5* (MGG_01808.5) was used as the endogenous constitutive reference gene. The relative quantification of each transcript was calculated by the $2^{-\Delta\Delta C_T}$ method (Livak and Schmittgen, 2001).

Immunoblot Analysis

Total proteins were isolated from vegetative hyphae as described (Bruno et al., 2004). Proteins separated on SDS-PAGE gels were transferred onto a nitrocellulose membrane with a Bio-Rad electroblotting apparatus. The expression and activation of Mps1 and Pmk1 MAP kinases were detected with the PhosphoPlus p44/42 MAP kinase antibody kit (Cell Signaling Technology). The horseradish peroxidase-conjugated secondary antibody and SuperSignal West Femto chemiluminescent substrate from Pierce were used for antigen antibody detections. The monoclonal anti-GFP (Roche), anti-FLAG (Sigma-Aldrich), and anti-actin (Sigma-Aldrich) antibodies were used at a 1:1000 to 1:2000 dilution for immunoblot analysis.

Generation of the Gene Replacement Mutants

The ligation-PCR approach (Zhao et al., 2004) was used to generate the *TIG1* gene replacement construct. The 0.9-kb upstream and 0.8-kb downstream flanking sequences of *TIG1* were amplified with primers F1/R1 and F2/R2 (see Supplemental Table 1 online). The resulting PCR products were digested with *FseI* and *AsclI*, respectively, and ligated with the *hph* gene from pCX63. After ligation, a 3.1-kb *TIG1* replacement construct was amplified with primers F1/R2 and transformed into protoplasts of Guy11 or 70-15. Hygromycin-resistant transformants were screened by PCR and confirmed by DNA gel blot analysis using the *TIG1* fragment, which was amplified with primers NF1/NR2, and the *hph* gene as probes (Figure 1A). For complementation, a 4.1-kb fragment containing the entire *TIG1* gene (with a 1.5-kb promoter region) was cloned into pYK11 (Park et al., 2006) and transformed into the *tig1* mutant KT-1.

The same approach was used to generate gene replacement constructs for other components of the *TIG1* complex. Primers used to amplify the flanking sequences of *HOS2*, *SNT1*, *SET3*, *HST1*, and *HOS4* are listed in Supplemental Table 1 online. The ligation-PCR products (Zhao et al., 2004) were transformed into protoplasts of Guy11, 70-15, or Ku80 (Villalba et al., 2008) to generate the *hos2*, *snt1*, *set3*, *hst1*, and *hos4* deletion mutants (Table 1). Putative knockout mutants were identified by PCR screens and confirmed by DNA gel blot analysis.

Construction of *TIG1*-GFP and *TIG1*-3xFLAG Fusion Constructs

To construct the *TIG1*-GFP fusion, the *TIG1* gene was amplified with primers TNG-F/TGFP-R (see Supplemental Table 1 online) and cotransformed with *XhoI*-digested pKB04 into *Saccharomyces cerevisiae* strain XK1-25 as described (Bourett et al., 2002; Bruno et al., 2004). Plasmid pSD11 was rescued from the resulting Trp⁺ yeast transformants, confirmed by sequence analysis to contain the *TIG1*-GFP fusion, and transformed into the *tig1* mutant KT-1. The resulting zeocin-resistant transformants, which exhibited wild-type colony morphology and growth rate, were analyzed by DNA gel blot hybridization. The expression of the *TIG1*-GFP fusion construct was observed under a Nikon E-800 epifluorescence microscope.

To generate the *TIG1*-3xFLAG fusion construct, the *TIG1* coding region was amplified with primers RPF and RPR (Supplemental Table 1). Primer RPR contains three copies of the FLAG epitope sequence followed by a termination codon. The resulting PCR products were co-transformed with *XhoI*-digested pDL2 (Bourett et al., 2002) into XK1-25 (Bruno et al., 2004). The *TIG1*-3xFLAG fusion vector was recovered from yeast transformants and transformed into 70-15.

Affinity Purification and Mass Spectrometry Analysis

About 150 to 200 mg of freshly harvested mycelia were resuspended in 2 mL of extraction buffer (50 mM Tris-HCl, pH 7.5, 100 mM NaCl, 50 mM NaF, 2 mM PMSF, 5 mM EDTA, 1 mM EGTA, 1% Triton X-100, and 10% glycerol) and 10 μ L of protease inhibitor cocktail (Sigma-Aldrich). After homogenization with a Biospec mini bead beater (Bruno et al., 2004), the lysate was centrifuged at full speed in a microcentrifuge for 20 min at 4°C. The supernatants were further centrifuged at 45,000 rpm at 4°C for 1 h to remove cell debris. About 50 μ L of anti-FLAG M2 beads (Sigma-Aldrich) were added to capture Tig1-interacting proteins, following the instructions of the manufacturer. After incubation at 4°C for 2 h, the beads were washed three times each with 500 μ L of lysis buffer, 50 mM TMAB (1 M trimethylammonium bicarbonate; Fluka), and sterile distilled water. Proteins binding to the beads were eluted with 150 μ L of 50 mM TMAB containing 0.1% Rapigest and digested with trypsin as described (Tao et al., 2005; Zhou et al., 2007). Tryptic peptides were analyzed by nanoflow liquid chromatography–tandem mass spectrometry on a high-resolution hybrid linear ion trap orbitrap mass spectrometer (LTQ-Orbitrap XL; ThermoFisher) coupled to an Agilent Nanoflow LC system. The tandem mass spectrometry data were queried against the National Center for Biotechnology Information nonredundant *M. oryzae* protein database using the SEQUEST algorithm (Tabb et al., 2001) on the Sorcerer IDA server (SageN). Putative *TIG1*-interacting genes were identified by MS analysis, and four biological replicates were performed. Proteins that bound nonspecifically to the anti-FLAG antibody had been identified in our preliminary studies (Supplemental Dataset 1) and were removed from the list of proteins copurified with Tig1-3xFLAG for further analysis (see Supplemental Table 2 online).

Co-IP Assays

The yeast gap repair approach (Bourett et al., 2002; Bruno et al., 2004) was used to generate the *SET3*-3xFLAG, *HOS2*-GFP, and *SET3*-GFP

fusion constructs. Primers used to amplify the *SET3* and *HOS2* genes are listed in Supplemental Table 1 online. The resulting fusion constructs were cotransformed into protoplasts of 70-15 in pairs. Transformants containing the *TIG1*-3xFLAG/*SET3*-GFP, *TIG1*-3xFLAG/*HOS2*-GFP, and *SET3*-3xFLAG/*HOS2*-GFP constructs were identified by PCR and confirmed by DNA gel blot hybridization. The expression of the GFP and 3xFLAG fusion proteins was further confirmed by immunoblot analyses. For co-IP assays, total proteins were isolated and incubated with the anti-FLAG M2 beads as described above. Proteins eluted from M2 beads were analyzed by immunoblot detection with the anti-FLAG (Sigma-Aldrich) and anti-GFP (Roche) antibodies.

Yeast Two-Hybrid Assays

The HybridZap2.1 yeast two-hybrid system (Stratagene) was used to assay protein–protein interactions. The *TIG1* ORF was cloned into pBD-GAL4 as the bait vector pSD17. The prey construct of *SET3* was generated with pAD-GAL4-2.1. The resulting bait and prey vectors were transformed into yeast strain YRG-2 (Stratagene) with the Alkali-Cation yeast transformation kit (MP Biomedicals). The Leu⁺ and Trp⁺ transformants were isolated and assayed for growth on SD-Trp-Leu-His medium and the expression of the LacZ reporter gene as described (Zhao et al., 2005). The positive and negative controls were provided in the HybridZap2.1 XR library construction kit (Stratagene).

HDAC Activity Assays

Protoplasts of Guy11, 70-15, Ku80, and the *tig1*, *hos2*, *set3*, and *snt1* mutants were resuspended to 4×10^8 protoplasts/mL in lysis buffer (10 mM Tris-HCl, pH 7.5, 10 mM NaCl, 15 mM MgCl₂, 250 mM sucrose, 0.5% Nonidet P-40, 0.1 mM EGTA, and 200 μ M PMSF). Nuclei and crude nuclear extracts were prepared from disrupted protoplasts as described (Ding et al., 2009) and assayed for HDAC activities with the HDAC activity assay kit (Cayman Chemical Company) following the instructions provided by the manufacturer. Fluorescent signals in samples of different mutants were detected with a plate reader (Synergy HT; Bio-TEK). The concentration of deacetylated compounds was calculated with the deacetylation standard curve and used to estimate HDAC activity (nmol/min/mL) using the formula provided in the HDAC activity assay kit.

Histone Acetylation Assays

Vegetative hyphae harvested from 100 mL of 2-d-old 5xYEG cultures were resuspended in 400 μ L lysis buffer (10 mM Tris-HCl, pH 7.4, 300 mM sorbitol, 600 mM NaCl, 5 mM MgCl₂, and 5 mM EDTA) with a mixture of protease and phosphatase inhibitors (1 μ g/mL of aprotinin, leupeptin, and pepstatin A, 1 mM PMSF, 1 μ M microcystin-LR, and 2 mM *p*-chloromercuriphenylsulfonic acid). Mycelia were homogenized with acid-washed glass beads in a Biospec minibead beater using three 40-s pulses applied at 1-min intervals on ice. The lysate was separated from the glass beads and centrifuged at 16,000g for 15 min at 4°C. The resulting supernatants containing whole-cell extracts were separated on 15% SDS-PAGE gels, transferred to a nitrocellulose membrane, and assayed for histone acetylation as described (Briggs et al., 2001). Monoclonal anti-H3 (Abcam) and anti-H3K18Ac (Abcam) antibodies were used for detection.

Accession Numbers

Sequence data for the *M. oryzae* genes from this article can be found in the GenBank/EMBL data libraries under the following accession numbers: *TIG1*, EDK00306; *SET3*, EDK04728; *SNT1*, EDJ98032; *HOS2*, EDK04649; *HST1*, EDJ98541; *HOS4*, EDK06449; *CYP1*, BAB59119; *HDA1*, EDK02244; *HOS3*, EDJ96334; *ACT1*, EDJ99269; *TUB1*, EDK02768; and *ILV5*, EDK04462. Others are as follows: the putative

ortholog of *TIG1* in *Neurospora crassa*, XP_963679; *FTL1* of *Fusarium graminearum*, XP_380508.

Supplemental Data

The following materials are available in the online version of this article.

Supplemental Figure 1. Alignment of Amino Acid Sequences of Tig1 and Its Putative Orthologs from *Neurospora crassa*, *Fusarium graminearum*, and *Saccharomyces cerevisiae* (Sif2).

Supplemental Figure 2. KT-2 and KT-4 Failed to Cause Typical Blast Lesions on Rice Leaves.

Supplemental Figure 3. The *Tig1* Mutant Triggered Enhanced Callose Deposition in Plant Cells.

Supplemental Figure 4. Immunoblot Analysis of the Expression and Immunoprecipitation of Tig1-3xFLAG Fusion Proteins with an anti-FLAG Antibody.

Supplemental Figure 5. Targeted Deletion of the *SNT1*, *SET3*, *HOS4*, *HOS2*, and *HST1* Gene.

Supplemental Figure 6. GFP Signals in the P_{RP27}-*TIG1*-GFP Transformant.

Supplemental Figure 7. Expression Patterns of *HOS3*, *HDA1*, and *CYP1*.

Supplemental Figure 8. Infection Assays with *hda1* and *hos3* Mutants.

Supplemental Table 1. PCR Primers Used in This Study.

Supplemental Data Set 1. *Magnaporthe oryzae* Proteins Nonspecifically Copurified with 3xFLAG.

ACKNOWLEDGMENTS

We thank Larry Dunkle and Charles Woloshuk at Purdue University for critical reading of this manuscript and Scott Briggs for assistance with histone acetylation assays. We also thank Xinhua Zhao for helpful discussions during this study and Mike Hasagawa and Dilap Shah for providing osmotin and MsDef1. This work was supported by a grant from the National Research Initiative of the USDA Cooperative State Research, Education, and Extension Service (2007-35319-102681) and the 111 Project from the Ministry of Education of China (B07049).

Received January 26, 2010; revised June 8, 2010; accepted July 7, 2010; published July 30, 2010.

REFERENCES

- Baidyaroy, D., Brosch, G., Ahn, J.H., Graessle, S., Wegener, S., Tonukari, N.J., Caballero, O., Loidl, P., and Walton, J.D. (2001). A gene related to yeast *HOS2* histone deacetylase affects extracellular depolymerase expression and virulence in a plant pathogenic fungus. *Plant Cell* **13**: 1609–1624.
- Bhambra, G.K., Wang, Z.Y., Soanes, D.M., Wakley, G.E., and Talbot, N.J. (2006). Peroxisomal carnitine acetyl transferase is required for elaboration of penetration hyphae during plant infection by *Magnaporthe grisea*. *Mol. Microbiol.* **61**: 46–60.
- Bourett, T.M., Sweigard, J.A., Czymbek, K.J., Carroll, A., and Howard, R.J. (2002). Reef coral fluorescent proteins for visualizing fungal pathogens. *Fungal Genet. Biol.* **37**: 211–220.
- Briggs, S.D., Bryk, M., Strahl, B.D., Cheung, W.L., Davie, J.K., Dent, S.Y.R., Winston, F., and Allis, C.D. (2001). Histone H3 lysine 4 methylation is mediated by Set1 and required for cell growth and rDNA silencing in *Saccharomyces cerevisiae*. *Genes Dev.* **15**: 3286–3295.
- Brosch, G., Loidl, P., and Graessle, S. (2008). Histone modifications and chromatin dynamics: A focus on filamentous fungi. *FEMS Microbiol. Rev.* **32**: 409–439.
- Bruno, K.S., Tenjo, F., Li, L., Hamer, J.E., and Xu, J.R. (2004). Cellular localization and role of kinase activity of *PMK1* in *Magnaporthe grisea*. *Eukaryot. Cell* **3**: 1525–1532.
- Cerna, D., and Wilson, D.K. (2005). The structure of sif2p, a WD repeat protein functioning in the *SET3* corepressor complex. *J. Mol. Biol.* **351**: 923–935.
- Chao, C.C.T., and Ellingboe, A.H. (1991). Selection for mating competence in *Magnaporthe grisea* pathogenic to rice. *Can. J. Bot.* **69**: 2130–2134.
- Chi, M.H., Park, S.Y., Kim, S., and Lee, Y.H. (2009). A novel pathogenicity gene is required in the rice blast fungus to suppress the basal defenses of the host. *PLoS Pathog.* **5**: e1000401.
- Clergeot, P.H., Gourgues, M., Cots, J., Laurans, F., Latorse, M.P., Pepin, R., Tharreau, D., Notteghem, J.L., and Lebrun, M.H. (2001). *PLS1*, a gene encoding a tetraspanin-like protein, is required for penetration of rice leaf by the fungal pathogen *Magnaporthe grisea*. *Proc. Natl. Acad. Sci. USA* **98**: 6963–6968.
- Coca, M.A., Damsz, B., Yun, D.J., Hasegawa, P.M., Bressan, R.A., and Narasimhan, M.L. (2000). Heterotrimeric G-proteins of a filamentous fungus regulate cell wall composition and susceptibility to a plant PR-5 protein. *Plant J.* **22**: 61–69.
- Cohen, T.J., Mallory, M.J., Strich, R., and Yao, T.P. (2008). Hos2p/Set3p deacetylase complex signals secretory stress through the Mpk1p cell integrity pathway. *Eukaryot. Cell* **7**: 1191–1199.
- Dean, R.A., et al. (2005). The genome sequence of the rice blast fungus *Magnaporthe grisea*. *Nature* **434**: 980–986.
- Ding, S.L., Mehrabi, R., Koten, C., Kang, Z.S., Wei, Y.D., Seong, K.Y., Kistler, H.C., and Xu, J.R. (2009). Transducin beta-like gene *FTL1* is essential for pathogenesis in *Fusarium graminearum*. *Eukaryot. Cell* **8**: 867–876.
- Ebbole, D.J. (2007). *Magnaporthe* as a model for understanding host-pathogen interactions. *Annu. Rev. Phytopathol.* **45**: 437–456.
- Fang, E.G.C., and Dean, R.A. (2000). Site-directed mutagenesis of the *MAGB* gene affects growth and development in *Magnaporthe grisea*. *Mol. Plant Microbe Interact.* **13**: 1214–1227.
- Ficner, R. (2009). Novel structural insights into class I and II histone deacetylases. *Curr. Top. Med. Chem.* **9**: 235–240.
- Flaherty, J.E., and Dunkle, L.D. (2005). Identification and expression analysis of regulatory genes induced during conidiation in *Exserohilum turcicum*. *Fungal Genet. Biol.* **42**: 471–481.
- Guenther, M.G., Barak, O., and Lazar, M.A. (2001). The SMRT and N-CoR corepressors are activating cofactors for histone deacetylase 3. *Mol. Cell. Biol.* **21**: 6091–6101.
- Jeon, J., Goh, J., Yoo, S., Chi, M.H., Choi, J., Rho, H.S., Park, J., Han, S.S., Kim, B.R., Park, S.Y., Kim, S., and Lee, Y.H. (2008). A putative MAP kinase kinase kinase, *MCK1*, is required for cell wall integrity and pathogenicity of the rice blast fungus, *Magnaporthe oryzae*. *Mol. Plant Microbe Interact.* **21**: 525–534.
- Kankanala, P., Czymbek, K., and Valent, B. (2007). Roles for rice membrane dynamics and plasmodesmata during biotrophic invasion by the blast fungus. *Plant Cell* **19**: 706–724.
- Kim, S., Park, S.Y., Kim, K.S., Rho, H.S., Chi, M.H., Choi, J., Park, J., Kong, S., Park, J., Goh, J., and Lee, Y.H. (2009). Homeobox transcription factors are required for conidiation and appressorium development in the rice blast fungus *Magnaporthe oryzae*. *PLoS Genet.* **5**: e1000757.
- Li, L., Ding, S.L., Sharon, A., Orbach, M., and Xu, J.R. (2007). Mir1 is highly upregulated and localized to nuclei during infectious hyphal

- growth in the rice blast fungus. *Mol. Plant Microbe Interact.* **20**: 448–458.
- Livak, K.J., and Schmittgen, T.D.** (2001). Analysis of relative gene expression data using real-time quantitative PCR and the 2(T)_{-Delta} Delta C) method. *Methods* **25**: 402–408.
- Mehrabi, R., Ding, S., and Xu, J.R.** (2008). MADS-box transcription factor Mig1 is required for infectious growth in *Magnaporthe grisea*. *Eukaryot. Cell* **7**: 791–799.
- Mitchell, T.K., and Dean, R.A.** (1995). The cAMP-dependent protein kinase catalytic subunit is required for appressorium formation and pathogenesis by the rice blast pathogen *Magnaporthe grisea*. *Plant Cell* **7**: 1869–1878.
- Mosquera, G., Giraldo, M.C., Khang, C.H., Coughlan, S., and Valent, B.** (2009). Interaction transcriptome analysis identifies *Magnaporthe oryzae* BAS1-4 as biotrophy-associated secreted proteins in rice blast disease. *Plant Cell* **21**: 1273–1290.
- Mou, Z.M., Kenny, A.E., and Curcio, M.J.** (2006). Hos2 and Set3 promote integration of Ty1 retrotransposons at tRNA genes in *Saccharomyces cerevisiae*. *Genetics* **172**: 2157–2167.
- Park, G., Bruno, K.S., Staiger, C.J., Talbot, N.J., and Xu, J.R.** (2004). Independent genetic mechanisms mediate turgor generation and penetration peg formation during plant infection in the rice blast fungus. *Mol. Microbiol.* **53**: 1695–1707.
- Park, G., Xue, C., Zhao, X., Kim, Y., Orbach, M., and Xu, J.R.** (2006). Multiple upstream signals converge on an adaptor protein Mst50 to activate the *PMK1* pathway in *Magnaporthe grisea*. *Plant Cell* **18**: 2822–2835.
- Pijnappel, W., Schaft, D., Roguev, A., Shevchenko, A., Tekotte, H., Wilm, M., Rigaut, G., Seraphin, B., Aasland, R., and Stewart, A.F.** (2001). The *Saccharomyces cerevisiae* SET3 complex includes two histone deacetylases, Hos2 and Hst1, and is a meiotic-specific repressor of the sporulation gene program. *Genes Dev.* **15**: 2991–3004.
- Ramamoorthy, V., Zhao, X.H., Snyder, A.K., Xu, J.R., and Shah, D.M.** (2007). Two mitogen-activated protein kinase signalling cascades mediate basal resistance to antifungal plant defensins in *Fusarium graminearum*. *Cell. Microbiol.* **9**: 1491–1506.
- Rispail, N., et al.** (2009). Comparative genomics of MAP kinase and calcium-calcineurin signalling components in plant and human pathogenic fungi. *Fungal Genet. Biol.* **46**: 287–298.
- Sesma, A., and Osbourn, A.E.** (2004). The rice leaf blast pathogen undergoes developmental processes typical of root-infecting fungi. *Nature* **431**: 582–586.
- Swiegard, J.A., Carroll, A.M., Farrall, L., Chumley, F.G., and Valent, B.** (1998). *Magnaporthe grisea* pathogenicity genes obtained through insertional mutagenesis. *Mol. Plant Microbe Interact.* **11**: 404–412.
- Tabb, D.L., Eng, J.K., and Yates, J.R.** (2001). Protein identification by SEQUEST. In *Proteome Research: Mass Spectrometry*, P. James, ed (Berlin: Springer-Verlag). 125–142.
- Talbot, N.J., Ebbole, D.J., and Hamer, J.E.** (1993). Identification and characterization of *MPG1*, a gene involved in pathogenicity from the rice blast fungus *Magnaporthe grisea*. *Plant Cell* **5**: 1575–1590.
- Tao, W.A., Wollscheid, B., O'Brien, R., Eng, J., Li, X., Bodenmiller, B., Watts, J., Hood, L., and Aebersold, R.** (2005). Quantitative phosphoproteome analysis using a dendrimer conjugation chemistry and mass spectrometry. *Nat. Methods* **2**: 591–598.
- Thines, E., Weber, R.W.S., and Talbot, N.J.** (2000). MAP kinase and protein kinase A-dependent mobilization of triacylglycerol and glyco-gen during appressorium turgor generation by *Magnaporthe grisea*. *Plant Cell* **12**: 1703–1718.
- Trojer, P., Brandtner, E.M., Brosch, G., Loidl, P., Galehr, J., Linzmaier, R., Haas, H., Mair, K., Tribus, M., and Graessle, S.** (2003). Histone deacetylases in fungi: novel members, new facts. *Nucleic Acids Res.* **31**: 3971–3981.
- Tucker, S.L., and Talbot, N.J.** (2001). Surface attachment and pre-penetration stage development by plant pathogenic fungi. *Annu. Rev. Phytopathol.* **39**: 385–419.
- Tucker, S.L., Thornton, C.R., Tasker, K., Jacob, C., Giles, G., Egan, M., and Talbot, N.J.** (2004). A fungal metallothionein is required for pathogenicity of *Magnaporthe grisea*. *Plant Cell* **16**: 1575–1588.
- Ubersax, J.A., Woodbury, E.L., Quang, P.N., Paraz, M., Blethrow, J.D., Shah, K., Shokat, K.M., and Morgan, D.O.** (2003). Targets of the cyclin-dependent kinase Cdk1. *Nature* **425**: 859–864.
- Urban, M., Bhargava, T., and Hamer, J.E.** (1999). An ATP-driven efflux pump is a novel pathogenicity factor in rice blast disease. *EMBO J.* **18**: 512–521.
- Vergne, E., Ballini, E., Marques, S., Mammari, B.S., Droc, G., Gaillard, S., Bourrot, S., DeRose, R., Tharreau, D., Notteghem, J.L., Lebrun, M.H., and Morel, J.B.** (2007). Early and specific gene expression triggered by rice resistance gene Pi33 in response to infection by *ACE1* avirulent blast fungus. *New Phytol.* **174**: 159–171.
- Viaud, M.C., Balhadere, P.V., and Talbot, N.J.** (2002). A *Magnaporthe grisea* cyclophilin acts as a virulence determinant during plant infection. *Plant Cell* **14**: 917–930.
- Villalba, F., Collemare, J., Landraud, P., Lambou, K., Brozek, V., Cirer, B., Morin, D., Bruel, C., Beffa, R., and Lebrun, M.H.** (2008). Improved gene targeting in *Magnaporthe grisea* by inactivation of *MgKU80* required for non-homologous end joining. *Fungal Genet. Biol.* **45**: 68–75.
- Wilson, R.A., Jenkinson, J.M., Gibson, R.P., Littlechild, J.A., Wang, Z.Y., and Talbot, N.J.** (2007). Tps1 regulates the pentose phosphate pathway, nitrogen metabolism and fungal virulence. *EMBO J.* **26**: 3673–3685.
- Wilson, R.A., and Talbot, N.J.** (2009). Under pressure: Investigating the biology of plant infection by *Magnaporthe oryzae*. *Nat. Rev. Microbiol.* **7**: 185–195.
- Xu, J.R., and Hamer, J.E.** (1996). MAP kinase and cAMP signaling regulate infection structure formation and pathogenic growth in the rice blast fungus *Magnaporthe grisea*. *Genes Dev.* **10**: 2696–2706.
- Xu, J.R., Staiger, C.J., and Hamer, J.E.** (1998). Inactivation of the mitogen-activated protein kinase *Mps1* from the rice blast fungus prevents penetration of host cells but allows activation of plant defense responses. *Proc. Natl. Acad. Sci. USA* **95**: 12713–12718.
- Xu, J.R., Zhao, X., and Dean, R.A.** (2007). From genes to genomes; A new paradigm for studying fungal pathogenesis in *Magnaporthe oryzae*. *Adv. Genet.* **57**: 175–218.
- Yoon, H.G., Chan, D.W., Huang, Z.Q., Li, J.W., Fondell, J.D., Qin, J., and Wong, J.M.** (2003). Purification and functional characterization of the human N-CoR complex: The roles of *HDAC3*, *TBL1* and *TBLR1*. *EMBO J.* **22**: 1336–1346.
- Zhang, X.-M., Chang, Q., Zeng, L., Gu, J., Brown, S., and Basch, R.S.** (2006). *TBLR1* regulates the expression of nuclear hormone receptor co-repressors. *BMC Cell Biol.* **7**: 31.
- Zhao, X., Kim, Y., Park, G., and Xu, J.R.** (2005). A mitogen-activated protein kinase cascade regulating infection-related morphogenesis in *Magnaporthe grisea*. *Plant Cell* **17**: 1317–1329.
- Zhao, X., Mehrabi, R., and Xu, J.-R.** (2007). Mitogen-activated protein kinase pathways and fungal pathogenesis. *Eukaryot. Cell* **6**: 1701–1714.
- Zhao, X.H., and Xu, J.R.** (2007). A highly conserved MAPK-docking site in Mst7 is essential for Pmk1 activation in *Magnaporthe grisea*. *Mol. Microbiol.* **63**: 881–894.
- Zhao, X.H., Xue, C., Kim, Y., and Xu, J.R.** (2004). A ligation-PCR approach for generating gene replacement constructs in *Magnaporthe grisea*. *Fungal Genet. Newsl.* **51**: 17–18.
- Zhou, F., Galan, J., Geahlen, R.L., and Tao, W.A.** (2007). A novel quantitative proteomics strategy to study phosphorylation-dependent peptide-protein interactions. *J. Proteome Res.* **6**: 133–140.